Chapter 5

On coupled systems of nonlinear singularly perturbed problems[4]

In this chapter, we consider the following coupled system of singularly perturbed first-order nonlinear differential equations

$$\boldsymbol{\mathcal{L}y} := \begin{pmatrix} \mathcal{L}_1\boldsymbol{y} \\ \mathcal{L}_2\boldsymbol{y} \end{pmatrix} := \begin{pmatrix} \varepsilon_1 y_1'(x) + \mathcal{R}_1(x, y_1(x), y_2(x)) \\ \varepsilon_2 y_2'(x) + \mathcal{R}_2(x, y_1(x), y_2(x)) \end{pmatrix} = \mathbf{0}, \quad x \in \mathcal{G} = (0,1], \tag{5.1}$$

with the given initial conditions

$$\begin{pmatrix} y_1(0) \\ y_2(0) \end{pmatrix} = \begin{pmatrix} \varphi_1 \\ \varphi_2 \end{pmatrix}, \tag{5.2}$$

where φ_1 and φ_2 are arbitrary constants. The small parameters multiplied with the first order derivative terms are called the 'perturbation parameters'. In general, they are distinct and such that $0 < \varepsilon_1, \varepsilon_2 \ll 1$. The nonlinear functions $\mathcal{R}_1(x, y_1, y_2),\ \mathcal{R}_2(x, y_1, y_2) \in C^2(\bar{\mathcal{G}} \times \mathbb{R}^2)$ with $\bar{\mathcal{G}} = \mathcal{G} \cup \{0\}$ satisfy the following assumptions:

$$\begin{cases} \dfrac{\partial \mathcal{R}_i}{\partial y_j} \le 0,\ i \ne j, \qquad \dfrac{\partial \mathcal{R}_i}{\partial y_j} \ge \gamma > 0,\ i = j, \quad i, j \in \{1, 2\}, \\ \displaystyle\sum_{r=1}^{2} \frac{\partial \mathcal{R}_i}{\partial y_r} \ge \delta > 0, \quad i = 1, 2. \end{cases}$$

Under these assumptions, (5.1)–(5.2) admits a unique solution (see [108, 133, 134]).

[4]This chapter contains material published in *Computational and Applied Mathematics*, 41 (83), 2022, doi: `https://doi.org/10.1007/s40314-022-01788-4`.

Best to our knowledge, no a posteriori analysis has been done so far for the model problem (5.1)–(5.2). Therefore, in this chapter, our objective is to provide the a posteriori error estimate in the maximum norm for the second-order discretization of (5.1)–(5.2) on an arbitrary non-uniform mesh. We remark that for simplicity we have considered the coupled system with two equations. However, the idea presented here can be easily extended to coupled systems with arbitrary number of equations.

The arrangement of this chapter is as follows: In Section 5.1, the stability of the continuous problem is discussed. The discretization of the problem is done in Section 5.2. A posteriori error analysis is provided in Section 5.3. In Section 5.4, the proposed numerical method is applied to a test problem, and the results are discussed in form of the tables and graphs. The chapter ends with some concluding remarks in Section 5.5.

5.1 Stability of the continuous problem

In this section, we derive stability estimate for the nonlinear system (5.1) with the initial condition (5.2), which will be needed in our a posteriori error analysis. We rewrite (5.1) in the linearized form as follows.

$$\hat{\boldsymbol{\mathcal{L}}}\boldsymbol{y} = \begin{pmatrix} \hat{\mathcal{L}}_1\boldsymbol{y} \\ \hat{\mathcal{L}}_2\boldsymbol{y} \end{pmatrix} = \begin{pmatrix} \varepsilon_1 y_1'(x) + p_1(x)y_1(x) + s_1(x)y_2(x) \\ \varepsilon_2 y_2'(x) + p_2(x)y_1(x) + s_2(x)y_2(x) \end{pmatrix} = \begin{pmatrix} R_1(x) \\ R_2(x) \end{pmatrix}, \quad x \in \mathcal{G}, \tag{5.3}$$

where

$$\begin{cases} p_j(x) = \dfrac{\partial \mathcal{R}_j}{\partial y_1}(x, \eta_j(x), \nu_j(x)), \ \ s_j(x) = \dfrac{\partial \mathcal{R}_j}{\partial y_2}(x, \eta_j(x), \nu_j(x)), \\ R_j(x) = -\mathcal{R}_j(x, 0, 0), \ \ j = 1, 2, \end{cases}$$

and $\eta_j(x), \nu_j(x), j = 1, 2$, and are intermediate values. Using problem assumptions, it follows that the operator $\hat{\boldsymbol{\mathcal{L}}}$ satisfies the following continuous maximum principle.

Lemma 5.1 (Continuous maximum principle)**.** *Let $\boldsymbol{y}$ be any function such that $\boldsymbol{y}(0) \geq \mathbf{0}$ and $\hat{\mathcal{L}}\boldsymbol{y} \geq \mathbf{0}$ on $\mathcal{G}$, then $\boldsymbol{y} \geq \mathbf{0}$ on $x \in \overline{\mathcal{G}}$.*

Proof. Suppose that the lemma is false. Then there exists at least one $x_\star$ such that

$$\min\{y_1(x_\star), y_2(x_\star)\} = \min\left\{\min_{x\in\overline{\mathcal{G}}} y_1(x), \min_{x\in\overline{\mathcal{G}}} y_2(x)\right\} < 0.$$

Clearly $x_\star \neq 0$. Also, $y_1'(x_\star) = 0$. Without loss of generality, let us assume that $y_1(x_\star) \leq y_2(x_\star)$. Using the problem assumptions, it is clear that $0 \leq -s_1(x_\star) < p_1(x_\star)$ and $0 \leq -s_2(x_\star) < p_2(x_\star)$. Therefore, we have $p_1(x_\star)y_1(x_\star) < -s_1(x_\star)y_2(x_\star)$. So $p_1(x_\star)y_1(x_\star)+s_1(x_\star)y_2(x_\star) < 0$. Hence, $\varepsilon_1 y_1'(x_\star)+p_1(x_\star)y_1(x_\star)+s_1(x_\star)y_2(x_\star) < 0$, which contradicts the hypothesis that $\hat{\mathcal{L}}\boldsymbol{y} \geq \mathbf{0}$. Thus, the proof is complete. □

The following stability estimate holds for the operator $\boldsymbol{\mathcal{L}}$.

Lemma 5.2. *For any two vector functions $\boldsymbol{z} = (z_1, z_2)^T$ and $\boldsymbol{w} = (w_1, w_2)^T$ such that $\boldsymbol{z}(0) = \boldsymbol{w}(0)$ and a bounded continuous piecewise vector function $\mathcal{T}$ satisfying*

$$\mathcal{T} = \boldsymbol{\mathcal{L}}\boldsymbol{z} - \boldsymbol{\mathcal{L}}\boldsymbol{w},$$

we have

$$\|\boldsymbol{z} - \boldsymbol{w}\|_\infty \leq C\|\boldsymbol{\mathcal{L}}\boldsymbol{z} - \boldsymbol{\mathcal{L}}\boldsymbol{w}\|_\infty.$$

Proof. Note that $(\boldsymbol{z}-\boldsymbol{w})(0) = \mathbf{0}$, and $\mathcal{T} = \mathcal{L}\boldsymbol{z}-\mathcal{L}\boldsymbol{w} = \hat{\mathcal{L}}(\boldsymbol{z}-\boldsymbol{w})$, where $\hat{\mathcal{L}}$ is defined by (5.3) with $p_j(x) = \dfrac{\partial \mathcal{R}_j}{\partial y_1}(x, \tilde{\eta}_j(x), \tilde{\nu}_j(x))$, $s_j(x) = \dfrac{\partial \mathcal{R}_j}{\partial y_2}(x, \tilde{\eta}_j(x), \tilde{\nu}_j(x)), j = 1, 2$, and $\tilde{\eta}_j(x), \tilde{\nu}_j(x), j = 1, 2$, are intermediate values. Now, consider the vector barrier function

$$\boldsymbol{\Psi}^{\pm}(x) = \frac{1}{\delta}\left\|\hat{\mathcal{L}}(\boldsymbol{z}-\boldsymbol{w})\right\|_{\infty} \pm (\boldsymbol{z}-\boldsymbol{w})(x), \quad x \in \overline{\mathcal{G}}.$$

Then, it can be readily shown that $\boldsymbol{\Psi}^{\pm}(0) \geq \mathbf{0}$ and $\hat{\mathcal{L}}\boldsymbol{\Psi}^{\pm}(x) \geq \mathbf{0}$ for $x \in \mathcal{G}$. Hence, Lemma 5.1 gives $\boldsymbol{\Psi}^{\pm}(x) \geq \mathbf{0}$ for $x \in \overline{\mathcal{G}}$. Consequently,

$$\begin{aligned}\|\boldsymbol{z}-\boldsymbol{w}\|_{\infty} &\leq \frac{1}{\delta}\left\|\hat{\mathcal{L}}(\boldsymbol{z}-\boldsymbol{w})\right\|_{\infty} \\ &\leq C\|\mathcal{L}\boldsymbol{z}-\mathcal{L}\boldsymbol{w}\|_{\infty}.\end{aligned}$$

. □

5.2 Discretization

We now describe the discretization of problem (5.1)–(5.2) on an arbitrary non-uniform mesh $\bar{\mathcal{G}}^N$, where $\bar{\mathcal{G}}^N = \{x_i : 0 = x_0 < \cdots < x_N = 1\}$ with step sizes $h_i = x_i - x_{i-1},\ i = 1, \ldots, N$. The interior points set is defined by $\mathcal{G}^N = \bar{\mathcal{G}}^N \backslash \{0\}$. On this mesh for a mesh function $\psi_i = \psi(x_i)$, we define

$$D^{-}\psi_i = \frac{\psi_i - \psi_{i-1}}{h_i},\ i = 1, \ldots, N.$$

Now, the discretized version of (5.1)–(5.2) is given by

$$\begin{aligned}\boldsymbol{L}^N\boldsymbol{Y}_i &= \begin{pmatrix}\mathrm{L}_1^N\boldsymbol{Y}_i \\ \mathrm{L}_2^N\boldsymbol{Y}_i\end{pmatrix} = \begin{pmatrix}\varepsilon_1 D^{-}Y_{1,i} + \beta_{1,i}^{l}\mathcal{R}_1(x_{i-1}, Y_{1,i-1}, Y_{2,i-1}) + \beta_{1,i}^{c}\mathcal{R}_1(x_i, Y_{1,i}, Y_{2,i}) \\ \varepsilon_2 D^{-}Y_{2,i} + \beta_{2,i}^{l}\mathcal{R}_2(x_{i-1}, Y_{1,i-1}, Y_{2,i-1}) + \beta_{2,i}^{c}\mathcal{R}_2(x_i, Y_{1,i}, Y_{2,i})\end{pmatrix} \\ &= \begin{pmatrix}0 \\ 0\end{pmatrix},\quad x_i \in \mathcal{G}^N \quad \text{and} \quad \boldsymbol{Y}_{\mathbf{0}} = \begin{pmatrix}\varphi_1 \\ \varphi_2\end{pmatrix},\end{aligned} \tag{5.4}$$

where the choice of the coefficients $\beta^l_{k,i}$ and $\beta^c_{k,i}$ is such that the discretization scheme satisfies a discrete maximum principle and is second order accurate. For $k = 1, 2$ and $i = 1, 2, \dots, N$, we consider

$$\begin{cases} \beta^l_{k,i} = 0.5,\ \beta^c_{k,i} = 0.5, & \text{if } \frac{\alpha_k h_i}{2} \le \varepsilon_k, \\ \beta^l_{k,i} = 0,\ \beta^c_{k,i} = 1, & \text{if } \frac{\alpha_k h_i}{2} > \varepsilon_k, \end{cases} \tag{5.5}$$

where $\alpha_k = \max\limits_{(x,y_1,y_2)\in\bar{\mathcal{G}}\times\mathbb{R}^2} \dfrac{\partial \mathcal{R}_k}{\partial y_k}$. This scheme was previously used in [2], where its a priori error analysis is performed, which requires information about the locations and widths of the layers. Here, we perform a posteriori error analysis of the discrete scheme (5.4). The a posteriori error estimate that we derive can be used in any adaptive moving mesh algorithm.

We rewrite the discrete problem (5.4) in the linearized form as follows:

$$\begin{aligned} \hat{\boldsymbol{L}}^N \boldsymbol{Y}_i &= \begin{pmatrix} \hat{\mathrm{L}}_1^N \boldsymbol{Y}_i \\ \hat{\mathrm{L}}_2^N \boldsymbol{Y}_i \end{pmatrix} \\ &= \begin{pmatrix} \varepsilon_1 D^- Y_{1,i} + \beta^l_{1,i}\left(a^{(1)}_{i-1} Y_{1,i-1} + b^{(1)}_{i-1} Y_{2,i-1}\right) + \beta^c_{1,i}\left(a^{(1)}_i Y_{1,i} + b^{(1)}_i Y_{2,i}\right) \\ \varepsilon_2 D^- Y_{2,i} + \beta^l_{2,i}\left(a^{(2)}_{i-1} Y_{1,i-1} + b^{(2)}_{i-1} Y_{2,i-1}\right) + \beta^c_{2,i}\left(a^{(2)}_i Y_{1,i} + b^{(2)}_i Y_{2,i}\right) \end{pmatrix} \\ &= \begin{pmatrix} \mathrm{F}_1 \\ \mathrm{F}_2 \end{pmatrix}, \end{aligned}$$

subject to the boundary condition

$$\boldsymbol{Y}_0 = \begin{pmatrix} \varphi_1 \\ \varphi_2 \end{pmatrix},$$

where $a^{(j)}_i = \dfrac{\partial \mathcal{R}_j}{\partial Y_1}(x_i, \zeta_{j,i}, \xi_{j,i})$, $b^{(j)}_i = \dfrac{\partial \mathcal{R}_j}{\partial Y_2}(x_i, \zeta_{j,i}, \xi_{j,i})$, $\mathrm{F}_j = -\beta^l_{j,i}\mathcal{R}_j(x_{i-1}, 0, 0) -$

$\beta^c_{j,i}\mathcal{R}_j(x_i,0,0)$, $j=1,2$, and $\zeta_{j,i},\xi_{j,i}, j=1,2$, are intermediate values. Equivalently, we can write

$$\begin{aligned}\hat{\boldsymbol{L}}^N\boldsymbol{Y}_i &= \begin{pmatrix}\hat{\mathrm{L}}_1^N\boldsymbol{Y}_i\\ \hat{\mathrm{L}}_2^N\boldsymbol{Y}_i\end{pmatrix}\\ &= \begin{pmatrix}\left(-\frac{\varepsilon_1}{h_i}+\beta^l_{1,i}a^{(1)}_{i-1}\right)Y_{1,i-1}+\left(\frac{\varepsilon_1}{h_i}+\beta^c_{1,i}a^{(1)}_{i}\right)Y_{1,i}+\beta^l_{1,i}b^{(1)}_{i-1}Y_{2,i-1}+\beta^c_{1,i}b^{(1)}_{i}Y_{2,i}\\ \left(-\frac{\varepsilon_2}{h_i}+\beta^l_{2,i}b^{(2)}_{i-1}\right)Y_{2,i-1}+\left(\frac{\varepsilon_2}{h_i}+\beta^c_{2,i}b^{(2)}_{i}\right)Y_{2,i}+\beta^l_{2,i}a^{(2)}_{i-1}Y_{1,i-1}+\beta^c_{2,i}a^{(2)}_{i}Y_{1,i}\end{pmatrix}\\ &= \begin{pmatrix}\mathrm{F}_1\\ \mathrm{F}_2\end{pmatrix}.\end{aligned}$$

Lemma 5.3 (Discrete maximum principle)**.** *For any vector mesh function* $\boldsymbol{Y}=(Y_1,Y_2)^T$ *satisfying* $\mathbf{Y}_0\geq\mathbf{0}$ *and* $\hat{\boldsymbol{L}}^N\boldsymbol{Y}_i\geq\mathbf{0}$, $1\leq i\leq N$, *we have* $\mathbf{Y}_i\geq\mathbf{0}$, $0\leq i\leq N$.

Proof. Under the problem assumptions, it can be observed that

$$\begin{cases}a^{(1)}_{i-1},a^{(1)}_i>0, & a^{(2)}_{i-1},\ a^{(2)}_i\leq 0,\\ b^{(1)}_{i-1},b^{(1)}_i\leq 0, & b^{(2)}_{i-1},b^{(2)}_i>0.\end{cases}\tag{5.6}$$

Let A be a matrix corresponding to the discrete operator $\hat{\boldsymbol{L}}^N$. Thus, we have

$$A\boldsymbol{Y}=\left(Y_{1,0},\hat{\mathrm{L}}_1^N\boldsymbol{Y}_1,\cdots,\hat{\mathrm{L}}_1^N\boldsymbol{Y}_N,Y_{2,0},\hat{\mathrm{L}}_2^N\boldsymbol{Y}_1,\cdots,\hat{\mathrm{L}}_2^N\boldsymbol{Y}_N\right)^T.$$

After taking (5.6) and the choice of coefficients $\beta^l_{k,i}$ & $\beta^c_{k,i}$ $(k=1,2)$ into consideration, it is easy to verify that the matrix A has non-positive off-diagonal entries and it is strictly diagonally dominant. Consequently, A is an $M-$matrix and has a positive inverse, i.e., $A^{-1}>0$ ([135]). Using this with $\boldsymbol{Y}_0\geq\mathbf{0}$ and $\hat{\boldsymbol{L}}^N\boldsymbol{Y}_i\geq\mathbf{0}$, $1\leq i\leq N$, we finally get $\boldsymbol{Y}_i\geq\mathbf{0}$ for $i=0,1,\cdots,N$. Thus, the proof is complete. □

An immediate consequence of the above lemma is the following stability bound.

Lemma 5.4. *The solution* $\boldsymbol{Y}$ *of the discrete problem (5.4) satisfies*

$$\|\boldsymbol{Y}\|_{\bar{\mathcal{G}}^N} \leq C \max\Big(\|\boldsymbol{Y}_0\|, \|\boldsymbol{F}\|_{\bar{\mathcal{G}}^N}\Big). \tag{5.7}$$

5.3 A posteriori error analysis

We now give a posteriori error analysis of the discrete scheme (5.4). Based on this we shall provide a suitable monitor function that can be used to construct layer-adapted meshes a posteriorly. Let $\widetilde{Y}_k(x)$ be a piecewise quadratic interpolation function of the solution $\{Y_{k,i}\}$ of discrete problem (5.4) for $x \in [x_{i-1}, x_i]$ as defined in [136]:

$$\widetilde{Y}_k(x) = Y_{k,i} + (x - x_i)D^-Y_{k,i} + \frac{1}{2}(x - x_{i-1})(x - x_i)D^-D^-Y_{k,i}. \tag{5.8}$$

Thus, $\widetilde{Y}_k(x_i) = Y_{k,i}$ and $\widetilde{Y}_k(x)$ is continuous in $\bar{\mathcal{G}}$ and quadratic in each $[x_{i-1}, x_i]$ and satisfy

$$[\widetilde{Y}_k(x)]' = D^-Y_{k,i} + (x - x_{i-\frac{1}{2}})D^-D^-Y_{k,i} \tag{5.9}$$

with $D^-D^-\psi_i = \dfrac{D^-\psi_i - D^-\psi_{i-1}}{h_i}$ and $x_{i-\frac{1}{2}} = \dfrac{x_{i-1} + x_i}{2}$. Here, we consider $D^-\psi_0 = 0$. We also define $q_k(x) = \mathcal{R}_k(x, \widetilde{Y}_1(x), \widetilde{Y}_2(x))$ and introduce $\widehat{q}_k(x)$ as its piecewise linear interpolant defined for $x \in [x_{i-1}, x_i]$ as

$$\widehat{q}_k(x) = q_{k,i} + (x - x_i)D^-q_{k,i}. \tag{5.10}$$

Hence, $q_{k,i} = q_k(x_i) = \mathcal{R}_k(x_i, Y_{1,i}, Y_{2,i})$.

Consequently, from (5.4), we have

$$\varepsilon_k D^- Y_{k,i} = \begin{cases} -\dfrac{q_{k,i-1}+q_{k,i}}{2}, & \text{if } \dfrac{h_i\alpha_k}{2} \le \varepsilon_k, \\ -q_{k,i}, & \text{if } \dfrac{h_i\alpha_k}{2} > \varepsilon_k. \end{cases} \tag{5.11}$$

In the next theorem we present the main result of this chapter as the a posteriori error estimate for the discrete scheme (5.4).

Theorem 5.1. *Let $\boldsymbol{y}$ be the solution of the system (5.1)–(5.2), $\boldsymbol{Y}$ be the approximate solution obtained from the discrete problem (5.4) and $\widetilde{\boldsymbol{Y}}$ be its piecewise quadratic interpolant defined in (5.8). Then, we have the following estimate*

$$\left\|\widetilde{\boldsymbol{Y}} - \boldsymbol{y}\right\|_\infty \le C \max_{1\le i\le N} h_i^2 \left\{ 1 + \sum_{k=1}^{2} \left(\left|D^- Y_{k,i}\right|^2 + \left|D^- D^- Y_{k,i}\right| + \left|D^- D^- q_{k,i}\right| \right) \right\}.$$

Proof. For $x \in (x_{i-1}, x_i)$, we have

$$\begin{aligned} \mathcal{L}_k \widetilde{Y}_k(x) - \mathcal{L}_k y_k(x) &= \varepsilon_k [\widetilde{Y}_k(x)]' + q_k(x) \\ &= \varepsilon_k [\widetilde{Y}_k(x)]' + \widehat{q}_k(x) + (q_k(x) - \widehat{q}_k(x)) \\ &= \varepsilon_k D^- Y_{k,i} + (x - x_{i-\frac{1}{2}})\varepsilon_k D^- D^- Y_{k,i} + \widehat{q}_k(x) + (q_k(x) - \widehat{q}_k(x)). \end{aligned}$$

Now, we discuss the remaining analysis in two cases; firstly when $\dfrac{h_i\alpha_k}{2} \le \varepsilon_k$:

$$\begin{aligned} \left|\mathcal{L}_k \widetilde{Y}_k(x) - \mathcal{L}_k y_k(x)\right| &= \Bigg| -\frac{q_{k,i-1}+q_{k,i}}{2} + (x - x_{i-\frac{1}{2}})\varepsilon_k D^- D^- Y_{k,i} + q_{k,i} + (x - x_i) D^- q_{k,i} \\ &\qquad + (q_k(x) - \widehat{q}_k(x)) \Bigg| \\ &= \Bigg| \frac{q_{k,i}-q_{k,i-1}}{2} + (x - x_{i-\frac{1}{2}})\varepsilon_k D^- D^- Y_{k,i} + (x - x_i) D^- q_{k,i} \\ &\qquad + (q_k(x) - \widehat{q}_k(x)) \Bigg| \\ &= \left| (x - x_{i-\frac{1}{2}}) D^- q_{k,i} + (x - x_{i-\frac{1}{2}})\varepsilon_k D^- D^- Y_{k,i} + (q_k(x) - \widehat{q}_k(x)) \right| \end{aligned}$$

$$
\begin{aligned}
&= \left|(x - x_{i-\frac{1}{2}})D^- \left(q_{k,i} - \frac{q_{k,i-1} + q_{k,i}}{2}\right) + (q_k(x) - \widehat{q}_k(x))\right| \\
&= \left|\frac{1}{2}(x - x_{i-\frac{1}{2}})D^- \left(h_i D^- q_{k,i}\right) + (q_k(x) - \widehat{q}_k(x))\right| \\
&\leq Ch_i^2\left|D^-D^-q_{k,i}\right| + |q_k(x) - \widehat{q}_k(x)|, \qquad (5.12)
\end{aligned}
$$

where we have used (5.9)–(5.11). Next, for the second case, *i.e.* when $\dfrac{h_i\alpha_k}{2} > \varepsilon_k$:

$$
\begin{aligned}
\left|\mathcal{L}_k\widetilde{Y}_k(x) - \mathcal{L}_k y_k(x)\right| &= \left| - q_{k,i} + (x - x_{i-\frac{1}{2}})\varepsilon_k D^-D^-Y_{k,i} + q_{k,i} + (x - x_i)D^-q_{k,i} + (q_k(x) - \widehat{q}_k(x))\right| \\
&= \left|(x - x_{i-\frac{1}{2}})D^-(\varepsilon_k D^-Y_{k,i}) + (x - x_i)D^-q_{k,i} + (q_k(x) - \widehat{q}_k(x))\right| \\
&= \left|(x - x_{i-\frac{1}{2}})D^-(-q_{k,i}) + (x - x_i)D^-q_{k,i} + (q_k(x) - \widehat{q}_k(x))\right| \\
&= \left|(x_i - x_{i-\frac{1}{2}})D^-(\varepsilon_k D^-Y_{k,i}) + (q_k(x) - \widehat{q}_k(x))\right| \\
&\leq Ch_i^2\left|D^-D^-Y_{k,i}\right| + |q_k(x) - \widehat{q}_k(x)|, \qquad (5.13)
\end{aligned}
$$

where we also have used (5.9)–(5.11). Now, it remains to find the bound of $|q_k(x) - \widehat{q}_k(x)|$. For this, we use the basic formula for linear interpolation error which includes the second order derivative of $q_k(x)$ given by

$$
\begin{aligned}
[q_k(x)]'' &= (\mathcal{R}_k)_{xx} + \sum_{l=1}^{2}(\mathcal{R}_k)_{y_l}(\widetilde{Y}_l)_{xx} + 2\sum_{l=1}^{2}(\mathcal{R}_k)_{xy_l}(\widetilde{Y}_l)_x + \sum_{l,m=1}^{2}(\mathcal{R}_k)_{y_l y_m}(\widetilde{Y}_l)_x(\widetilde{Y}_m)_x \\
&= (\mathcal{R}_k)_{xx} + \sum_{l=1}^{2}(\mathcal{R}_k)_{y_l}D^-D^-Y_{l,i} + 2\sum_{l=1}^{2}(\mathcal{R}_k)_{xy_l}\left[D^-Y_{l,i} + (x - x_{i-\frac{1}{2}})D^-D^-Y_{l,i}\right] \\
&\quad + \sum_{l,m=1}^{2}(\mathcal{R}_k)_{y_l y_m}\left[D^-Y_{l,i} + (x - x_{i-\frac{1}{2}})D^-D^-Y_{l,i}\right]\left[D^-Y_{m,i} + (x - x_{i-\frac{1}{2}})D^-D^-Y_{m,i}\right].
\end{aligned}
$$

Thus, using the standard linear interpolant error estimate [126], we have

$$
|q_k(x) - \widehat{q}_k(x)| \leq \frac{h_i^2}{2}\sup_{x\in(x_{i-1},x_i)}[q_k(x)]''
$$

$$\leq \quad Ch_i^2\left\{1+\sum_{k=1}^{2}\left|D^-D^-Y_{k,i}\right|+\sum_{k=1}^{2}\left|D^-Y_{k,i}\right|^2\right\}. \tag{5.14}$$

Now, on combining (5.12), (5.13) and (5.14), we obtain

$$\left\|\boldsymbol{\mathcal{L}}\widetilde{\boldsymbol{Y}}-\boldsymbol{\mathcal{L}}\boldsymbol{y}\right\|_\infty \leq C\max_{1\leq i\leq N} h_i^2\left\{1+\sum_{k=1}^{2}\left|D^-Y_{k,i}\right|^2+\sum_{k=1}^{2}\left|D^-D^-Y_{k,i}\right|+\sum_{k=1}^{2}\left|D^-D^-q_{k,i}\right|\right\}.$$

Thus, by using the stability result from Lemma 5.2 we get the desired result. $\square$

5.4 Numerical results

This section is devoted to the numerical validation of our theoretical result. To this end, we consider a test example from [2, 108], which is solved for various small values of the perturbation parameters and discretization parameters. We use Newton's method [127] to solve the system of nonlinear equations corresponding to the discrete scheme. The stopping criterion for the iterations is taken as

$$\max\left\{\left\|Y_1^{(n)}-Y_1^{(n-1)}\right\|_{\bar{\mathcal{G}}^N}, \left\|Y_2^{(n)}-Y_2^{(n-1)}\right\|_{\bar{\mathcal{G}}^N}\right\} \leq TOL,$$

where TOL is the maximum tolerable error for the solution. We consider a simple moving mesh algorithm originally due to De Boor [40]. Starting from a uniform mesh the algorithm aims to construct a mesh that solves

$$\mathcal{P}_i h_i = \frac{1}{N}\sum_{i=1}^{N}\mathcal{P}_i h_i,\ i=1,\ldots,N, \tag{5.15}$$

where $\mathcal{P}$ is the discrete monitor function which is chosen from the a posteriori error estimate obtained in Theorem 5.1:

$$\mathcal{P}_i = 1 + \sum_{k=1}^{2} \left|D^- Y_{k,i}\right| + \sum_{k=1}^{2} \left|D^- D^- Y_{k,i}\right|^{\frac{1}{2}} + \sum_{k=1}^{2} \left|D^- D^- q_{k,i}\right|^{\frac{1}{2}}. \tag{5.16}$$

However, it is observed in [43] that it is good enough to use a relaxed form of the equidistribution principle given by

$$\mathcal{P}_i h_i \le \frac{\rho}{N} \sum_{i=1}^{N} \mathcal{P}_i h_i, \quad i = 1, \ldots, N, \tag{5.17}$$

where $\rho > 1$ is the user chosen relaxing constant introduced to manage the number of iterations and the accuracy during the mesh generation process. If one considers a small value of ρ, the solution will be more accurate and the number of iteration will be more. To obtain the adaptive mesh points x_i and the numerical solution $Y_{k,i}$ we need to solve (5.17) and (5.4) simultaneously. The moving mesh algorithm that we considered here has been previously used for many classes of singularly perturbed problems, see e.g. [43, 76, 137, 138]. The convergence of this algorithm has been studied in [43] for a nonlinear convection-diffusion equation and in [131] for a regular boundary problem.

Example 5.1. *Consider the problem*

$$\begin{cases} \varepsilon_1 y_1' + 3y_1 - \frac{1}{4}e^{-y_1^2} - y_2 - x^2 + 1 = 0, \quad x \in \mathcal{G}, \\ \varepsilon_2 y_2' + 4y_2 - \cos y_2 - y_1 - e^x = 0, \quad x \in \mathcal{G}, \\ y_1(0) = 0, \quad y_2(0) = 0. \end{cases} \tag{5.18}$$

We solve this example using the Algorithm 4. We take $TOL = 10^{-8}$ as the error of tolerance in the iterative scheme and $\rho = 1.1$ as the stopping constant in the mesh

Algorithm 4: Mesh generation algorithm

Step 1. Initialize the mesh iteration ($r = 0$) as the uniform mesh $x_i^{(0)} = \frac{i}{N},\ i = 0, \ldots, N$.

Step 2. Compute the solution $\boldsymbol{Y}_{k,i}^{(r)}$ from (5.4) on the mesh $\{x_i^{(r)}\}$.

Step 3. Evaluate $\mathcal{P}_i^{(r)}$ from (5.16) for $i = 1, \ldots, N$ taking $D^- q_{k,0} = 0$, and compute $\Psi_i^{(r)} = \sum_{j=1}^{i} h_j^{(r)} \mathcal{P}_j^{(r)}$.

Step 4. **Stopping criterion:** if $\max_{1 \le i \le N} h_i^{(r)} \mathcal{P}_i^{(r)} \le \rho \frac{\Psi_N^{(r)}}{N}$ holds, go to Step 6, else go to Step 5.

Step 5. Define $Q_i = i \frac{\Psi_N^{(r)}}{N}$ for $i = 0, \ldots, N$. Generate a new mesh $\{x_i^{(r+1)}\}$ by interpolation of the points $(\Psi_i^{(r)}, x_i^{(r)})$ and evaluating at Q_i for $i = 0, 1, \ldots, N$. Return to Step 2 setting $r = r + 1$.

Step 6. Consider $\{x_i^{(r)}\}$ and $Y_{k,i}^{(r)}$ as the adaptive mesh and solution, respectively, and Stop.

---

generation algorithm. For $\varepsilon_1 = 10^{-4},\ \varepsilon_2 = 10^{-2}$ and $N = 64$ we plot the solution in Figure 5.1 showing the presence of boundary layers.

Since the exact solution of this problem is not known, we use the double mesh principle for calculation of errors and rates of convergence. In this idea, the mesh with N discretization points is bisected and the solution obtained at these two meshes denoted by $\boldsymbol{Y}^N$ and $\boldsymbol{Y}^{\boldsymbol{2N}}$, respectively, are compared to obtain the maximum pointwise errors using the formula

$$F_k^{\varepsilon_1,\varepsilon_2,N} = \max_{1 \le i \le N} \left| Y_{k,i}^N - Y_k^{2N}(x_i) \right|, \quad k = 1, 2.$$

Then, the uniform errors are given by $F_k^N = \max_{\varepsilon_1,\varepsilon_2} \{F_k^{\varepsilon_1,\varepsilon_2,N}\}$, and the corresponding uniform rates of convergence are calculated by $\varrho_k^N = \log_2 \left(F_k^N / F_k^{2N} \right)$.

In Tables 5.1 and 5.2, we present the maximum pointwise errors and corresponding

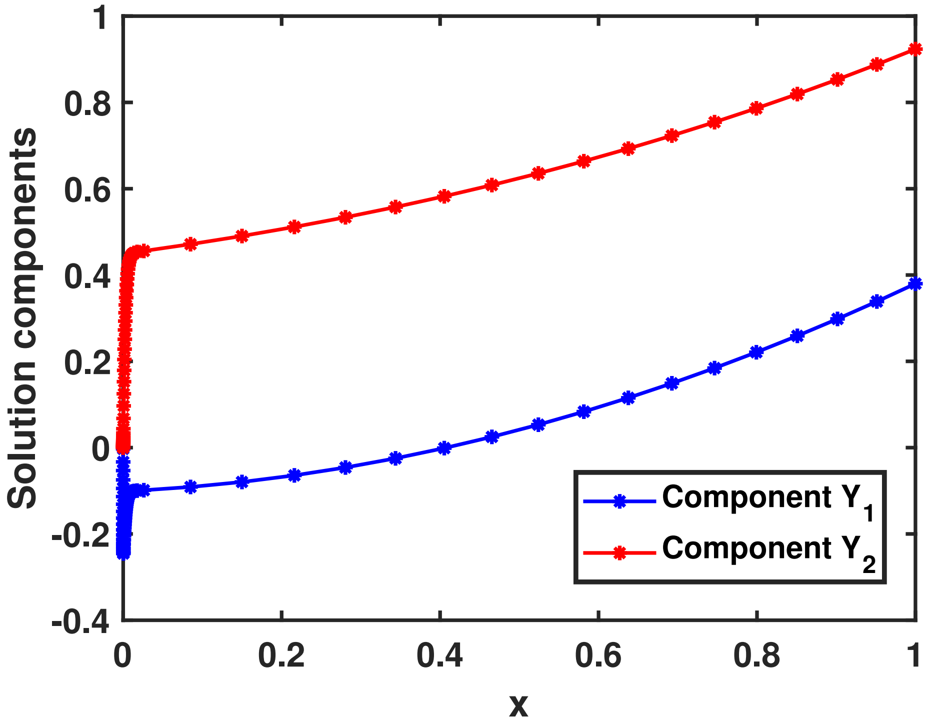

FIGURE 5.1: Numerical solution plot for $\varepsilon_1 = 10^{-4}$, $\varepsilon_2 = 10^{-2}$ and $N = 64$.

$\varepsilon_1{=}2^{-12-3\xi}$ $\varepsilon_2{=}10^{-\xi}$	$N = 32$	$N = 64$	$N = 128$	$N = 256$	$N = 512$	$N = 1024$
$\xi = 1$	8.1027e-04	1.6025e-04	4.0249e-05	1.0209e-05	2.7403e-06	6.5559e-07
	2.3381	1.9933	1.9791	1.8975	2.0635	
$\xi = 2$	7.1018e-04	1.7076e-04	4.2452e-05	1.0766e-05	2.7296e-06	6.9035e-07
	2.0562	2.0081	1.9793	1.9797	1.9833	
$\xi = 3$	7.2593e-04	1.7439e-04	4.3362e-05	1.0802e-05	2.7305e-06	6.9038e-07
	2.0575	2.0078	2.0052	1.9840	1.9837	
$\xi = 4$	1.2380e-03	1.7712e-04	4.3087e-05	1.0830e-05	2.7309e-06	6.8874e-07
	2.8052	2.0394	1.9922	1.9876	1.9874	
$\xi = 5$	9.1439e-04	1.7654e-04	4.3430e-05	1.0832e-05	2.7344e-06	6.8709e-07
	2.3728	2.0232	2.0034	1.9859	1.9927	
$\xi = 6$	7.7820e-04	1.7806e-04	4.4956e-05	1.0897e-05	2.7253e-06	6.8501e-07
	2.1278	1.9858	2.0446	1.9994	1.9922	
F_1^N	1.2380e-03	1.7806e-04	4.4956e-05	1.0897e-05	2.7403e-06	6.9038e-07
ϱ_1^N	2.7976	1.9858	2.0446	1.9915	1.9889	

TABLE 5.1: Errors and convergence rates for component y_1.

rates of convergence for components y_1 and y_2, respectively. The last two lines in each table represent the uniform errors and rates of convergence. These numerical observations evidently approve the uniform convergence of the method with second order. Further, we compare the performance of the proposed method with the method in [2]. The comparative results are reported in Table 5.3. In [2], the scheme is analyzed on Shishkin and Bakhvalov meshes constructed using a priori information. In contrast, the proposed approach does not require any a priori information. Further, from Table 5.3, it is evident that the proposed method is superior

$\varepsilon_1{=}2^{-12-3\xi}$ $\varepsilon_2{=}10^{-\xi}$	$N = 32$	$N = 64$	$N = 128$	$N = 256$	$N = 512$	$N = 1024$
$\xi = 1$	6.1578e-04	3.3313e-04	3.6003e-05	8.9580e-06	2.2336e-06	5.5652e-07
	0.8863	3.2099	2.0069	2.0038	2.0049	
$\xi = 2$	9.3014e-04	1.7263e-04	4.2792e-05	1.0817e-05	4.2673e-06	1.9987e-06
	2.4298	2.0122	1.9840	1.3419	1.0942	
$\xi = 3$	7.4143e-04	1.7951e-04	4.4098e-05	1.1105e-05	2.8146e-06	7.1302e-07
	2.0463	2.0253	1.9895	1.9802	1.9809	
$\xi = 4$	8.6189e-04	1.8228e-04	4.4237e-05	1.2095e-05	2.8252e-06	7.1499e-07
	2.2414	2.0428	1.8709	2.0979	1.9824	
$\xi = 5$	1.3143e-03	1.8168e-04	6.1096e-05	1.1163e-05	3.6836e-06	7.1416e-07
	2.8548	1.5723	2.4524	1.5995	1.3668	
$\xi = 6$	9.6998e-04	3.0793e-04	6.5481e-05	1.6484e-05	2.8229e-06	7.1246e-07
	1.6553	2.2335	1.9900	2.5458	1.9863	
F_2^N	1.3143e-03	3.3313e-04	6.5481e-05	1.6484e-05	4.2673e-06	7.1499e-07
ϱ_2^N	1.9801	2.3469	1.9900	1.9915	2.5773	

TABLE 5.2: Errors and convergence rates for component y_2.

to the method [2]. Table 5.4 shows how the stopping constant ρ affects the maximum errors, convergence rates, and the number of iterations needed to obtain the approximate solution. Here, we set $\varepsilon_1 = 2^{-20}$ and $\varepsilon_2 = 10^{-5}$. One can observe that although the errors and the rate of convergence don't differ much irrespective of different values of ρ, the number of iterations required to obtain the adaptive mesh decreases with an increase in ρ.

We also give log-log plot in Figure 5.2 between the maximum pointwise errors and the number of mesh intervals for both the components taking $N = 64$ and for two different values of perturbation parameters: $\varepsilon_1 = 2^{-15}, \varepsilon_2 = 2^{-10}$ and $\varepsilon_1 =$

Mesh		Number of intervals N					
		$N=32$	$N=64$	$N=128$	$N=256$	$N=512$	$N=1024$
Shishkin mesh [2]	y_1	2.4905e-03	8.8932e-04	3.0198e-04	9.8360e-05	3.1092e-05	9.5942e-06
		1.4857	1.5582	1.6183	1.6615	1.6963	
	y_2	7.1032e-03	2.4669e-03	8.1892e-04	2.6540e-04	8.3768e-05	2.5795e-05
		1.5258	1.5909	1.6256	1.6637	1.6993	
Bakhvalov mesh [2]	y_1	5.9339e-02	2.9794e-03	7.6709e-04	1.9805e-04	5.0516e-05	1.2727e-05
		4.3159	1.9576	1.9535	1.9711	1.9888	
	y_2	2.9622e-02	7.5570e-03	1.7895e-03	5.0932e-04	1.2869e-04	3.2410e-05
		1.9708	2.0783	1.8129	1.9847	1.9894	
Present method	y_1	1.2380e-03	1.7806e-04	4.4956e-05	1.0897e-05	2.7403e-06	6.9038e-07
		2.7976	1.9858	2.0446	1.9915	1.9889	
	y_2	1.3143e-03	3.3313e-04	6.5481e-05	1.6484e-05	4.2673e-06	7.1499e-07
		1.9801	2.3469	1.9900	1.9915	2.5773	

TABLE 5.3: Comparison of uniform errors and convergence rates of the method [2] and the present method.

	Number of intervals N						ρ
	$N=32$	$N=64$	$N=128$	$N=256$	$N=512$	$N=1024$	
No. of Iterations	126	58	45	14	10	9	
y_1	6.6233e-04	1.4374e-04	3.3641e-05	7.6271e-06	1.9810e-06	4.9419e-07	
	2.2041	2.0952	2.1410	1.9449	2.0031		1.1
y_2	4.9346e-04	1.1659e-04	3.7027e-05	8.4180e-06	2.1429e-06	5.4246e-07	
	2.0814	1.6549	2.1370	1.9739	1.9820		
No. of Iterations	17	8	9	9	9	7	
y_1	7.5059e-04	1.5111e-04	3.2964e-05	7.6515e-06	1.8080e-06	4.9347e-07	
	2.3124	2.1967	2.2046	1.9839	1.9331		1.5
y_2	5.4712e-04	2.2350e-04	4.2759e-05	8.5380e-06	2.1542e-06	5.4316e-07	
	1.2916	2.3860	2.3243	1.9867	1.9877		
No. of Iterations	13	8	8	7	6	6	
y_1	7.0895e-04	1.5111e-04	3.0943e-05	7.9548e-06	2.0424e-06	4.7374e-07	
	2.2300	2.2879	1.9597	1.9616	2.1081		2.0
y_2	4.9478e-04	2.2350e-04	3.3016e-05	8.4523e-06	2.1722e-06	5.4491e-07	
	1.1465	2.7590	1.9657	1.9602	1.9951		
No. of Iterations	8	8	6	6	6	5	
y_1	9.3425e-04	1.5111e-04	3.4582e-05	7.7802e-06	2.0424e-06	5.2434e-07	
	2.6282	2.1275	2.1521	1.9295	1.9617		3.0
y_2	9.5993e-04	2.2350e-04	3.6673e-05	8.7346e-06	2.1722e-06	8.1774e-07	
	2.1027	2.6075	2.0699	2.0076	1.4094		
No. of Iterations	8	7	6	6	5	5	
y_1	9.3425e-04	1.8727e-04	3.4582e-05	7.7802e-06	1.9891e-06	5.2434e-07	
	2.3187	2.4370	2.1521	1.9677	1.9235		5.0
y_2	9.5993e-04	1.5816e-04	3.6673e-05	8.7346e-06	2.3271e-06	8.1774e-07	
	2.6016	2.1086	2.0699	1.9082	1.5088		

TABLE 5.4: Uniform errors and convergence rates on the a posteriori mesh for different values of ρ for Example 5.1.

$2^{-30}, \varepsilon_2 = 2^{-20}$. The slope of this plot also confirms the second order convergence of the method. The solution adaptive nature of the a posteriori mesh is shown in Figure 5.3. The trajectory of moving mesh through iterations and final position of

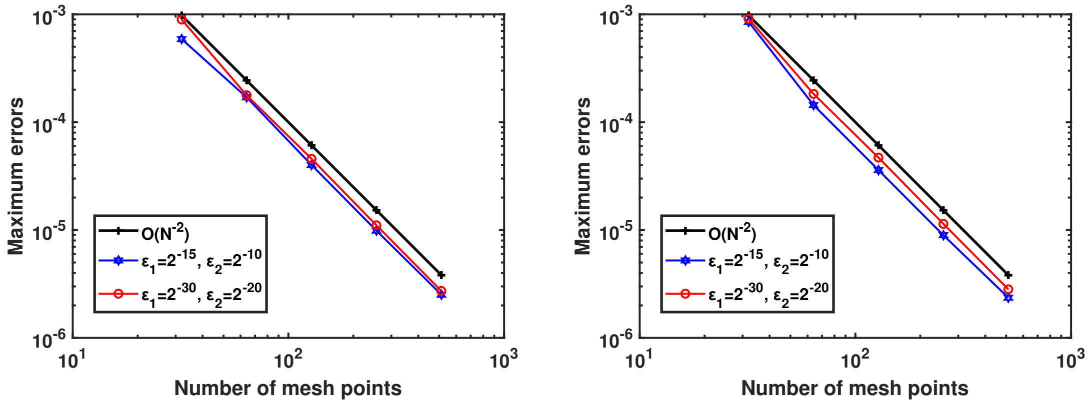

(A) Component y_1 (B) Component y_2

FIGURE 5.2: Log-log plots between maximum errors and number of mesh points.

the solution adaptive mesh are given in Figures 5.3A and 5.3B, respectively. The condensing of mesh points towards the boundary $x = 0$ shows the solution adaptivity of a posteriori mesh.

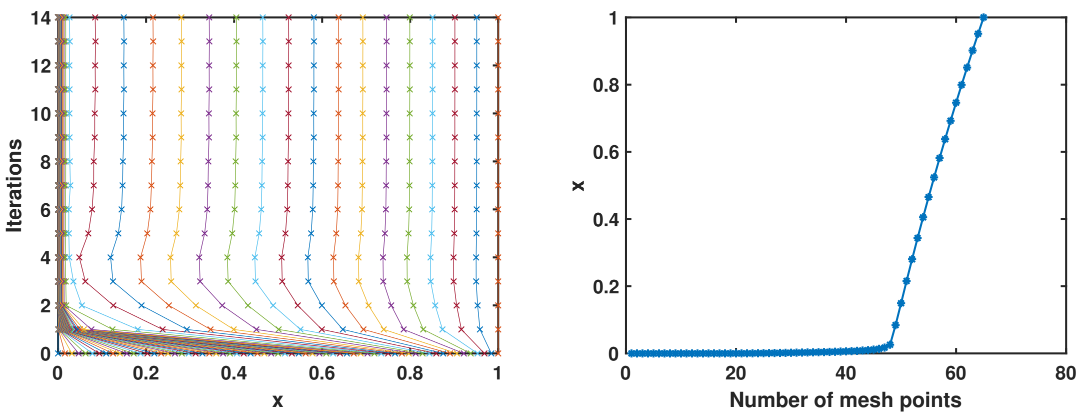

(A) Mesh trajectory with iterations (B) Mesh points location

FIGURE 5.3: Movement of mesh points through few iterations and the final adapted position of mesh points for $N = 64$ and $\varepsilon_1 = 10^{-4},\ \varepsilon_2 = 10^{-2}$.

5.5 Conclusions

A coupled system of nonlinear singularly perturbed differential equations of first order is considered that exhibits overlapping layers. The discretization of the problem is done using a hybrid finite difference scheme, for which a posteriori error analysis is given in the maximum norm. Using the derived a posteriori error estimate a moving mesh procedure is developed using a simple moving mesh algorithm. The numerical results are presented and the method is shown to produce optimal second order accurate results. Further, it is observed that the proposed method can be easily extended for a system of arbitrary number of equations.